research articles Journal of proteome research

Proteome Profiling in the Rat Harderian Gland

Jae-Won Yang,[†] Leila Afjehi-Sadat,[†] Ellen Gelpi,[‡] Markus Kunze,[§] Harald Höger,[||] Jan Fleckner,[⊥] Johannes Berger,[§] and Gert Lubec*,[†]

Department of Pediatrics, Medical University of Vienna, Vienna, Austria, Institute of Neurology, Medical University of Vienna, Vienna, Austria, Center for Brain Research, Medical University of Vienna, Vienna, Austria, Institute for Laboratory Animal Science, Medical University of Vienna, Vienna, Austria, and Department of Molecular Genetics, Novo Nordisk A/S, Bagsværd, Denmark

Received March 8, 2006

The Harderian gland is an orbital gland located behind the ocular bulb in most terrestrial vertebrates probably functioning for production of lipid secretion to protect the eye. We herein present a protein reference database of the rat Harderian gland that may serve as analytical tool for future proteomic work, report lipid and porphyrin handling cascades, address sequence conflicts and report structures that have not been so far described by proteomics methods.

Keywords: novel protein • hypothetical proteins • lipid metabolism • porphyrin metabolism • sequence conflicts • profiling • reference database

Introduction

Although known for about three hundred years, functions of the Harderian gland (HG) have not been fully elucidated.[1,2] Research is also hampered by the fact that studies were not focusing on one species, but rather were carried out in a variety of species including guinea pig, hamsters, mice, rabbits, gerbils, and others, and there is no reason to believe that functions among species are comparable.

A most intriguing observation is that HGs are secreting lipids and that the organ per se consists of 20% lipids by weight.[1] Speculations about the function of lipid secretion include lubrication of the eye,[3] thermoregulation,[4,5] function as hydrophobic carrier and vehicle for pheromones.[6]

Hais and co-workers[7] reported preliminary thin-layer chromatographical data on the rat HG following an article on lipids of the rabbit HG in 1967.[8]

Isolation and identification of an alkyldiacylglycerol containing isovaleric acid in rabbits was reported shortly afterward and this observation characterized a major specific lipid in HG in other species.[9] In the rat HG, the first paper on unsaturated wax esters as specific lipids was shown by Murawski and Jost.[10] Bareggi and co-workers carried out systematic work describing glycolipids,[11] phospholipids[12] and neutral lipids[13] in the rodent HG. Tvrzicka and co-workers[14] carried out thin-layer chromatographical studies followed by flame ionization experiments an wax esters along with polar lipids were the major HG lipids detected and the content of fatty acids determined by GC−MS revealed the presence of specific positional isomers monoenoic acids. The detection of mono-ethers and mono-esters by GC−MS was communicated by Harvey:[15] Forty-eight lipidic compounds were analyzed. Major constituents were fatty acids with chain lengths from 12 to 22 carbon atoms and fatty alcohols derived from wax esters. Most of them were unsaturated at the omega-7 position. The presence of ether chains was confirmed and these were straight-chain saturated, unsaturated and branched. Cholesterol was the only sterol observed.

The main lipid in the rat and most HG of other species is 1-alkyl-2,3-diacylglycerol. Enzymes and other proteins for the synthesis of these lipids as well as for their handling were not reported in the rat HG, and we therefore aimed to provide basic information on the corresponding structures in the rat HG.

Another chemical class has been attracting the attention: porphyrins are present in the HG in the order of microgram amounts per mg of tissue.[16] Park and co-workers[17] have shown porphyrin fluorescence in the cytoplasm of glandular cells. Protoporphyrin IX was determined as the major porphyrin in hamster HGs[18] and some porphyrins are present as glycoconjugates.[19] The role of porphyrins in the HG and for the organism per se has not been elucidated yet and is mainly speculative although sexual dimorphism and gonadal endocrine regulation of porphyrins[20−24] have been reported. Adaptation to season and light may represent another possible function physiological of porphyrins in the HG.[25,26] Providing general proteome information on porphyrin metabolising and handling enzymes was therefore another goal of the study.

The advent of the state-of-the-art proteomic technologies allows generation of protein maps and reference databases, unambiguously identifying proteins independent of antibody

* To whom correspondence should be addressed. Department of Pediatrics, Medical University of Vienna, Waehringer Guertel 18-20, A-1090 Vienna, Austria. Tel: + 43-1-40 400 3215. Fax: + 43-1-40 400 3194. E-mail: gert.lubec@meduniwien.ac.at.

[†] Department of Pediatrics, Medical University of Vienna.

[‡] Institute of Neurology, Medical University of Vienna.

[§] Center for Brain Research, Medical University of Vienna.

[||] Institute for Laboratory Animal Science, Medical University of Vienna.

[⊥] Department of Molecular Genetics, Novo Nordisk A/S.

10.1021/pr060082b CCC: $33.50

Published on Web 06/06/2006

availability and specificity. Herein, we used a robust method, two-dimensional gel electrophoresis with in-gel digestion of protein spots followed by mass spectrometric analysis and identification of proteins by specific software. In this study, identification of HG proteins allows creation of a reference map for lipid, porphyrin handling and metabolic proteins, characterize hypothetical proteins and sequence conflicts were addressed.

Experimental Procedures

Rat Harderian Gland. All animal procedures met the guidelines of the European Union for care and management of experimental animals. Sprague−Dawley rats, male and 8 days old were sacrificed for the experiments by decapitation and the HGs were rapidly dissected and snap-frozen in liquid nitrogen immediately. The HGs were kept at −80 °C until biochemical assays were performed. The freezing chain was never interrupted until analysis.

Two-Dimensional Gel Electrophoresis (2-DE). HGs were ground in liquid nitrogen and suspended in 1 mL of sample buffer consisting of 7 M urea, 2 M thiourea, 4% CHAPS, 10 mM DTT, 1 mM EDTA, 1 mM PMSF, and a mixture of protease inhibitors (Roche Diagnostics, Mannheim, Germany). After sonication for approximately 15 s, the suspension was left at room temperature for 1 h and centrifuged at 14 000 × *g* for 60 min at 12 °C. Desalting was done with Ultrafree-4 centrifugal filter unit (Millipore, Bedford, MA). The protein content of the supernatant was determined by the Coomassie blue method. 2-DE was performed essentially as reported.[27] Samples of 1 mg protein were applied on immobilized pI 3−10 nonlinear gradient strips (Amersham Bioscience, Uppsala, Sweden). Focusing started at 200 V and the voltage was gradually increased to 8000 V at 4 V/min and kept constant for a further 3 h (approximately 150 000 Vh in total). The second-dimensional separation was performed on 9−16% gradient SDS polyacrylamide gels. After protein fixation for 12 h in 50% methanol and 10% acetic acid, the gels were stained with colloidal Coomassie blue (Novex, San Diego, CA) for 8 h and excess of dye was washed out from the gels with distilled water. Molecular masses were determined by running standard protein markers (Bio-Rad Laboratories, Hercules, CA) covering the range 10−250 kDa. p*I* values were used as given by the supplier of the immobilized pH gradient strips.

MALDI-TOF and MALDI-TOF/TOF−Mass Spectrometry (MS). Spots were excised with a spot picker (PROTEINEER sp, Bruker Daltonics, Bremen, Germany), placed into 96-well microtiter plates and in-gel digestion and sample preparation for MALDI analysis were performed by an automated procedure (PROTEINEER dp, Bruker Daltonics).[27,28] Briefly, spots were excised and washed with 10 mM ammonium bicarbonate and 50% acetonitrile in 10 mM ammonium bicarbonate. After washing, gel plugs were shrunk by addition of acetonitrile and dried by blowing out the liquid through the pierced well bottom. The dried gel pieces were reswollen with 40 ng/μL trypsin (Promega, Madison, WI) in enzyme buffer (consisting of 5 mM octyl β-D-glucopyranoside (OGP) and 10 mM ammonium bicarbonate) and incubated for 4 h at 30 °C. To improve sequence coverage, uroporphyrinogen decarboxylase (URO-D) spots were further digested with chymotrypsin (100 ng/μL; Roche) and Asp-N (12.5 ng/μL; Roche) for 4 h at 30 °C, respectively. Peptide extraction was performed with 10 μL of 1% TFA in 5 mM OGP. Extracted peptides were directly applied onto a target (AnchorChip, Bruker Daltonics) that was loaded with α-cyano-4-hydroxy-cinnamic acid (Bruker Daltonics) matrix thinlayer. The mass spectrometer used in this work was an Ultraflex TOF/TOF (Bruker Daltonics) operated in the reflector for MALDI-TOF peptide mass fingerprint (PMF) or LIFT mode for MALDI-TOF/TOF with a fully automated mode using the FlexControl software. An accelerating voltage of 25 kV was used for PMF. Calibration of the instrument was performed externally with $[M + H]^+$ ions of angiotensin I, angiotensin II, substance P, bombesin, and adrenocorticotropic hormones (clip 1−17 and clip 18−39). Each spectrum was produced by accumulating data from 200 consecutive laser shots for PMF. Those samples which were analyzed by PMF from MALDI-TOF were additionally analyzed using LIFT-TOF/TOF MS/MS from the same target with two MS/MS modes: laser-induced dissociation (LID) and collision-induced dissociation (CID).[29] In the LID−MS/MS mode using a long-lifetime N_2 laser, all ions were accelerated to 8 kV under conditions promoting metastable fragmentation in the TOF1 stage. After selection of jointly migrating parent and fragment ions in a timed ion gate, ions were lifted by 19 kV to high potential energy in the LIFT cell. After further acceleration of the fragment ions in the second ion source, their masses could be simultaneously analyzed in the reflector with high sensitivity. In addition to the LID−MS/MS mode, a high-energy CID mode was adapted for distinguishing leucine and isoleucine by their different side-chain fragmentation. Argon gas as a collision gas was used and about 1500 shots were used to achieve spectra. PMF and LIFT spectra were interpreted with the Mascot search engine (versions 2.0 and 2.1; Matrix Science Ltd, London, UK). Database searches, through Mascot, using combined PMF and MS/MS data sets were performed via BioTools (versions 2.2 and 3.0) software. A mass tolerance of 25 ppm (50 ppm for the chymotrypsin and Asp-N digests) and MS/MS tolerance of 0.5 Da and 0 or 1 missing cleavage site (max. 2 sites for the chymotrypsin and Asp-N digests) were allowed and carbamidomethylation of cysteine and oxidation of methionine residues were considered. The probability score calculated by the software was used as criterion for correct identification (http://www.matrixscience.com/help/scoring-help.html). Nonidentified spots by Mascot database searches were then applied to ProFound database (http://prowl.rockefeller.edu/profound_bin/WebProFound.exe) with a maximum mass tolerance of 25 ppm and 0 or 1 missing cleavage site. The identification with significant Z score and similarity of observed pI/molecular weight (MW) to theoretical p*I*/MW values was accepted from the ProFound search results.

Unmatched peaks in the Mascot database search for adipocyte plasma membrane-associated protein (APMAP) and hypothetical protein Q8CC88 were further analyzed by de Novo sequencing analysis. MS/MS spectra were sequenced de Novo using BioTool 2.2 software with full de Novo sequencing extension and high scoring candidate sequences for MS/MS spectra were then submitted to MS BLAST sequence similarity search (http://dove.embl-heidelberg.de/Blast2/msblast.html), which was based on the most likely de Novo sequences. Protein identification significance was judged using the MS BLAST scoring algorithm.[30,31]

Western Blot Analysis. Two-dimensional gels or 12.5% homogeneous ExcelGel SDS gel (Amersham Bioscience, Uppsala, Sweden) separating proteins from the rat HG were electrotransferred onto PVDF membranes (MilliPore, Bedford, MA). After incubation in blocking solution (10 mM Tris-HCl, pH 7.5, 150 mM NaCl, 0.05% Tween 20 and 5% nonfat dry milk),

membranes were incubated with antibodies against APMAP,[32] catechol *O*-methyltransferase (COMT; Chemicon, Temecula, CA), monoglyceride lipase (MGL; Cayman, Ann Arbor, MI), sterol carrier protein-2 (SCP2; provided by Prof. Dr. K. Wirtz, Utrecht, Netherlands)[33] and acyl CoA oxidase (provided by Dr. G. Hoefler, Graz, Austria)[34] for 2 h at room temperature. After washing three times for 10 min with washing solution (0.3% Tween 20 in TBS), membranes were incubated with a horseradish peroxidase (HPR)-conjugated secondary anti-rabbit IgG antibody for 1 h at room temperature. Membranes were washed three times for 10 min and antigen−antibody complexes were visualized by ECL reagents Western Lightning (PerkinElmer Life Sciences, Boston, MA) or SuperSignal West Pico (Pierce, Rockford, IL) on an X-ray film.

Immunohistochemistry. Eyes and retroocular tissue including HG and single free sebaceous gland of five rats were fixed in buffered formaldeyde solution (4,5%) and embedded in paraffin. Tissue sections were cut at a thickness of 3−5 μm. Sections were stained with hematoxylin-eosin (H&E). Immunohistochemistry comprised primary antibodies against MGL (rabbit, polyclonal, dilution 1:100, Cayman), COMT (rabbit, polyclonal, dilution 1:100, Chemicon), and vimentin (mouse, monoclonal, dilution 1:50, DAKO, Glostrup, Denmark). Antigen retrieval was performed by boiling sections in citrate buffer at pH 6 for 10 min. Antibody binding was visualized with the ChemMate detection kit (DAKO), and diaminobenzidine was used as chromogen. Control of antibody specificity included omission or substitution of the primary antibodies by nonspecific, isotype-matched antibodies.

Characterization of Hypothetical Proteins. Bioinformatic database searches were performed for the characterization of hypothetical proteins:[31] InterPro (http://www.ebi.ac.uk/InterProScan/) and Pfam (http://pfam.wustl.edu/hmmsearch.shtml) databases for detecting of domains, ScanProsite (http://www.expasy.org/prosite/) for motif predictions, InterWeaver (http://interweaver.i2r.a-star.edu.sg/) and STRING (http://string.embl.de/) databases for prediction of interacting partner and SignalP 3.0 Server (http://www.cbs.dtu.dk/services/SignalP/) and PSORT II (http://psort.ims.u-tokyo.ac.jp/form2.html) for prediction of signal peptides and subcellular localizations. Local sequence alignment results were based on different BLAST database searches, FASTA (http://www.ebi.ac.uk/fasta33/) and MPsrch (http://www.ebi.ac.uk/MPsrch/). RPS-, PSI-, and BLASTp were linked at BLAST website (http://www.ncbi.nlm.nih.gov/BLAST/). ClustalW (http://www.ebi.ac.uk/clustalw/) was used for multiple sequence alignment searches. Secondary structure prediction and 3D structure prediction was based on Phyre database search results (http://www.sbg.bio.ic.ac.uk/~phyre/).

ATPase Activity Assay. After the samplewas separated on 2D gel, the gel was reversibly stained by negative staining (E-Zinc, Rockford, IL) leaving the proteins unstained and discernible against dark background. Proteins of interest were detected and excised from 2D gel. Protein elution from the gel matrix was performed by a Nanosep centrifugal device (300K molecular weight cut off (MWCO); Pall Life Sciences, Ann Arbor, MI) in the presence of elution buffer (0.25 M Tris-HCl buffer, pH 6.8; 0.1% (w/v) SDS). Protein eluant was concentrated using a new Nanosep centrifugal device equipped with a 3K-MWCO and 6 M guanidine in renaturation buffer (100 mM KCl, 12.5 mM $MgCl_2$, 25 mM HEPES (pH 7.6), 0.1 mM EDTA, 20 mM β-mercaptoethanol and 10% (v/v) Glycerol) was treated in a Nanosep centrifugal device. The solution was then exchanged and permitted to renature with renaturation buffer.

ATPase activity of the recovered protein was measured by colorimetric assay kit (Innova Biosciences, Cambridge, UK) based on the malachite green assay.[35] Protein was serially diluted for the assay and a standard curve was determined using P_i to calculate enzyme activity according to the manufacturer's protocol.

Results

Identification of Proteins in Rat Harderian Gland. The protein extracts (1 mg) of pooled rat HG, was separated by 2-DE and several hundred spots were visualized by colloidal Coomassie blue staining. After in-gel digestion, 644 protein spots corresponding to 281 different proteins were unambiguously identified using MALDI-TOF and TOF/TOF with Mascot database and 41 proteins with 55 spots (including 24 proteins which were not presented in Mascot results) additionally identified with ProFound database from nonidentified protein spots by Mascot database searches (see Supporting Information Table 1 online). Finally, 699 protein spots corresponding to 305 individual proteins were identified in rat HG and assigned to the 2D gel images. Figure 1 shows selected proteins referred in the Results and Discussion sections and the 2D maps with all identified proteins can be found as Supporting Information Figure 1 online. Data obtained from MALDI−MS(/MS) analysis are presented in Supporting Information Table 1 online including matched peptide numbers (matches) or sequence coverage (%), theoretical p*I*/MW values, number of identified spots and statistically significant Mascot scores or Z scores from ProFound.

MALDI−MS/MS analysis showed unambiguous identification of proteins in the rat HG including a series of interesting proteins which has tissue specific expression or tumor-related properties and has not been reported in the HG. Nucleoside diphosphate kinase A (Q05982), scinderin (Q7TQ08), catechol *O*-methyltransferase (COMT; P22734), adipocyte plasma membrane-associated protein (APMAP; Q9D7N9) and HIV-1 tat interactive protein 2 (Q99KN6) were unambiguously identified in the rat HG with MALDI−MS/MS analysis (See Supporting Information Table 1 online and Supporting Information Figure 2 online). One MS/MS spectrum at m/z 3291 in identified APMAP, which could not be assigned using Mascot database search, was analyzed by de Novo sequencing (see Supporting Information Figure 3 online).

Among these proteins, the expression of APMAP and COMT was validated by Western blot analysis. APMAP was reported as a novel glycosylated integral plasma membrane-associated protein involved in the cross-talk of mature adipocytes with the environment.[32] We identified 3 spots of APMAP at 43 and 40 kDa on 2D gel and additionally 35 kDa protein by Western blot analysis. The soluble COMT was detected at 21 kDa and the low expressed membrane bound COMT was observed at 24 kDa (Figure 2A).

Expression of Lipid Metabolic Proteins in Harderian Gland. Identified proteins in the rat HG were categorized into several functional groups based on their representative biological roles (see Supporting Information Table 1 online and Figure 3). Among these proteins, 33 proteins (107 proteins spots) involved in lipid metabolism were identified (Table 1), which includes

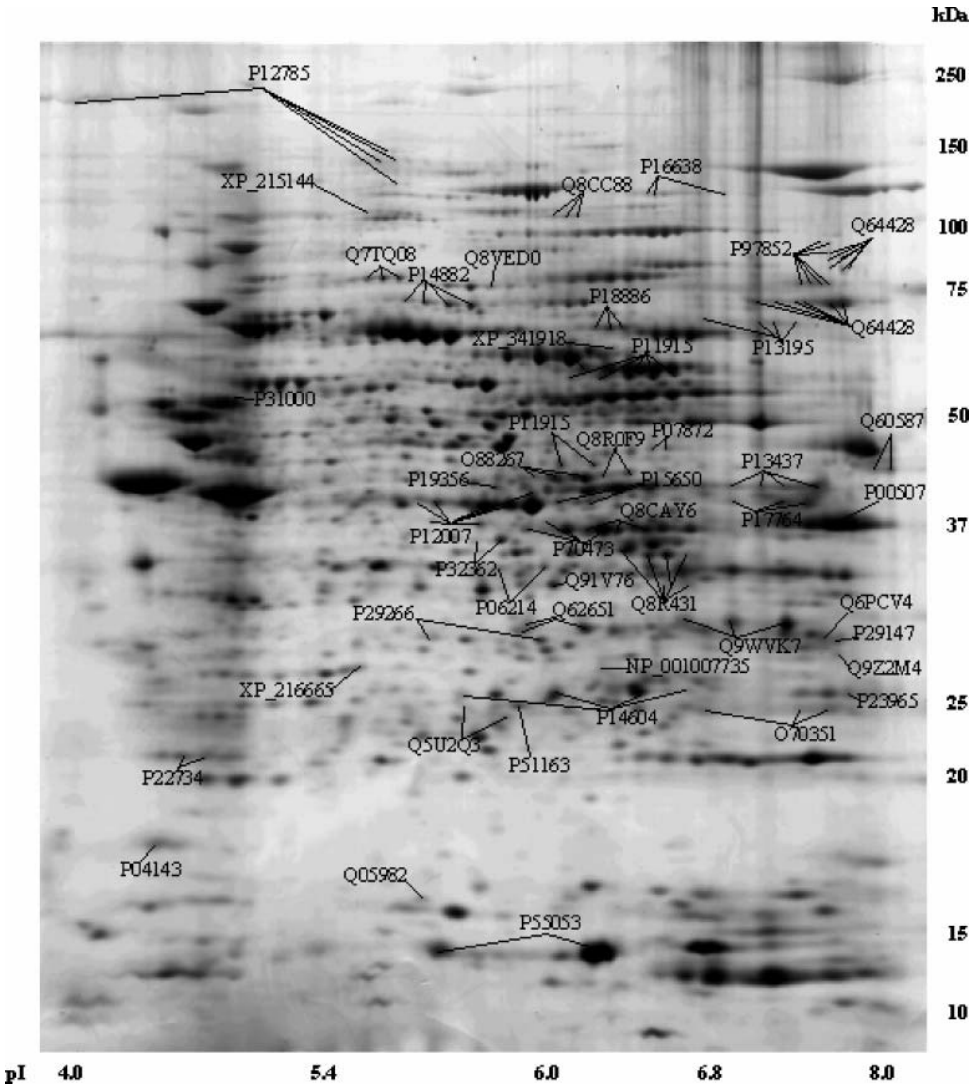

Figure 1. Part of 2D map from the constructed 2D reference map of the rat HG (see Supporting Information Figure 1 online). This map represents proteins involved in lipid metabolism and porphyrin synthesis and some interesting proteins referred in the results and discussion sections. Identified proteins are designated by their Swiss-Prot or NCBI accession number. The names of the proteins are listed in Table 1 and Supporting Information Table 1 online.

monoglyceride lipase (MGL; Q8R431), sterol carrier protein 2 (SCP2; nonspecific lipid-transfer protein; P11915), acyl CoA oxidase (AOX; P07872), and thyroid hormone-inducible hepatic protein (spot 14; P04143). We confirmed the expression of MGL in HG by Western blot analysis. MGL was observed at 31 and 35 kDa in agreement with MALDI-TOF/TOF result (see Supporting Information Figure 4 online) and additionally detected at 70 kDa on Western blot (Figure 2A). To confirm the expression patterns of SCP2 and AOX, we applied Western blot to both 2D gel (so-called 2D-Western blot) and 1D gel. Seven spots of SCP2 were identified at 58 and 44 kDa on 2D gel by mass spectrometry. With antibody against SCP2, 5 protein spots at 58 kDa were detected as identified above by MALDI analysis and each of 2 spots was additionally observed at 52 and 13 kDa on 2D-Western blot. Two spots of AOX were observed at 48 kDa by 2D-Western blotting which was in accordance with the identification from MALDI analysis (Figure 2B). We identified highly expressed epidermal-type fatty acid-binding protein (E-FABP; P55053), which has not been described in the HG, on 2D gel from the rat HG by MALDI−MS/MS (see Supporting Information Table 1 online and Supporting Information Figure 2 online).

Immunohistochemistry. Paraffin sections contained ocular structures including bulbus, small fragments of optic nerve, muscle and fat tissue, small sebaceous glands, and a big retroocular gland, the Harderian gland. Immunohistochemistry for COMT and MGL showed strong labeling of epithelial cells of both the Harderian and sebaceous glands. Vimentin (P31000) was expressed in mesenchymal tissue including fibroblasts and vessel walls (Figure 4).

Conflicting Sequence of Uroporphyrinogen Decarboxylase. Uroporphyrinogen decarboxylase (URO-D; P32362) is one of five identified porphyrin metabolic proteins in the rat HG. (see Supporting Information Table 1 online). Two spots of URO-D were identified with 16 and 11 matched peptides using trypsin in-gel digestion. To confirm this identification, 9 precursor ions were selected for further MS/MS analysis using LID and CID mode. Six out of nine peptides were assigned in rat URO-D

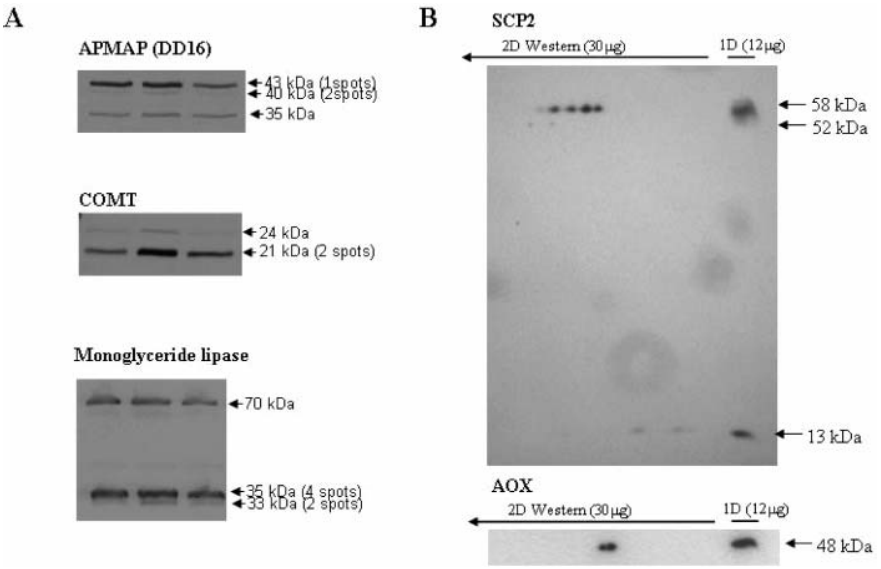

Figure 2. Western blot patterns of adipocyte plasma membrane-associated protein (APMAP), catechol *O*-methyltransferase (COMT) and monoglyceride lipase (MGL) in the rat HG. Denatured proteins (12 μg) were separated on 12.5% homogeneous gels and transferred onto PVDF membrane and subsequently reacted with antibodies against APMAP (1:1000), COMT (1:2000) and MGL (1:100), respectively. Number of spots given in parentheses represents the identified spots number at the same MW by mass spectrometry (A). 2D-Western blot patterns of SCP2 and AOX in the rat HG. 2DE was performed with 30 μg and when it applied to 9−16% gradient SDS-PAGE as second dimensional separation, 12 μg of protein was loaded at the edge for 1D-Western blot. 2D- and 1D-Western blot were performed on the same membrane with anti-SCP2 (1:5000) and anti-AOX (1:5000) antibodies, respectively.

Table 1. Lipid Metabolic Proteins Identified from the Rat HG

		Fatty Acid Metabolism
beta oxidation of fatty acids	O70351	3-hydroxyacyl-CoA dehydrogenase type II
	P13437	3-ketoacyl-CoA thiolase, mitochondrial
	*P*23965	3,2-trans-enoyl-CoA isomerase, mitochondrial [Precursor]
	P15650	acyl-CoA dehydrogenase, long-chain specific, mitochondrial [Precursor]
	XP_341918	similar to medium-chain acyl-CoA synthetase
	P18886	carnitine O-palmitoyltransferase II
	P14604	enoyl-CoA hydratase, mitochondrial [Precursor]
	NP_001007735	enoyl Coenzyme A hydratase domain containing 1
	P97852	peroxisomal multifunctional enzyme type 2 (MFE−2)
	Q9WVK7	short chain 3-hydroxyacyl-CoA dehydrogenase, mitochondrial [Precursor]
	Q64428	trifunctional enzyme alpha subunit, mitochondrial [Precursor]
	Q60587	trifunctional enzyme beta subunit, mitochondrial [Precursor]
	P07872	acyl-coenzyme A oxidase 1, peroxisomal
odd numbered fatty acids	Q8VED0	mut protein [Methylmalonyl-CoA mutase]
	P14882	propionyl-CoA carboxylase alpha chain
unsaturated fatty acids	Q6PCV4	2,4-dienoyl CoA reductase 1, mitochondrial
	Q62651	delta3,5-delta2,4-dienoyl-CoA isomerase, mitochondrial [Precursor]
	Q9Z2M4	peroxisomal 2,4-dienoyl-CoA reductase
branched chain/bile acids		
	P70473	alpha-methylacyl-CoA racemase
	O88267	cytosolic acyl coenzyme A thioester hydrolase
	P12007	isovaleryl-CoA dehydrogenase, mitochondrial [Precursor]
	P11915	sterol carrier protein 2 (nonspecific lipid-transfer protein) peroxidomal
synthesis	P16638	ATP-citrate synthase
	P12785	fatty acid synthase
		Lipid Binding/Transport
	P00507	aspartate aminotransferase, mitochondrial [Precursor]
	P55053	fatty acid-binding protein, epidermal (E-FABP)
	Q8R0F9	SEC14-like protein 4
lipogenesis		
	P04143	thyroid hormone-inducible hepatic protein
lipolysis		
	Q8R431	monoglyceride lipase
		Ketone Body Formation
	P29266	3-hydroxyisobutyrate dehydrogenase, mitochondrial [Precursor]
	P29147	D-beta-hydroxybutyrate dehydrogenase, mitochondrial [Precursor]
	P17764	acetyl-CoA acetyltransferase, mitochondrial [Precursor]
	Q8CAY6	acetyl-CoA acetyltransferase, cytosolic

and 2 MS/MS results were not assigned with database in rat taxonomy but existed in other taxonomies as conserved sequences (see Supporting Information Figure 5 online). One MS/MS spectrum given no significance using Mascot database

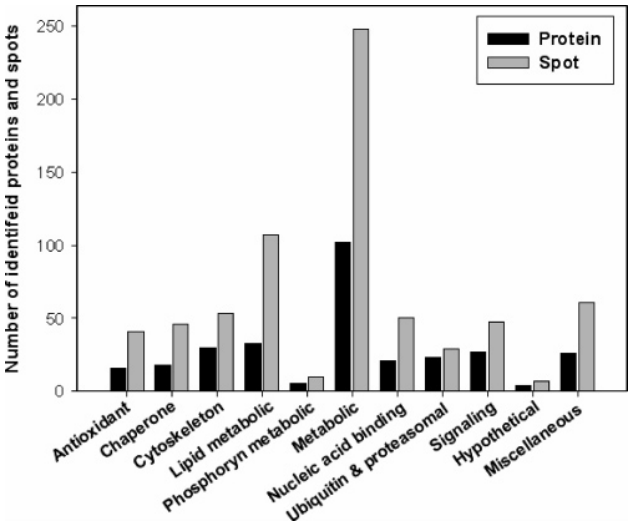

Figure 3. Distribution of the identified proteins and protein spots from the rat HG in functional groups.

search was sequenced by de Novo sequencing and assigned the sequence YLPEFR to rat URO-D at m/z 824.415. The sequence coverage of URO-D was increased from 38.2% to 76.1% by applying chymotrypsin and Asp-N for the MS and MS/MS analysis and one more conflicting amino acid was identified by MS/MS in a chymotrypsin digested peptide. (Figure 5 and Table 2).

Characterization of Hypothetical Proteins (HPs) in HG. Mass spectrometrical analysis of the identified rat HG proteome showed four identified hypothetical proteins: hypothetical P-loop containing nucleotide triphosphate hydrolases structure containing protein(HP Q8CC88), hypothetical LOC363016 (Q5U2Q3), RIKEN cDNA 4931406C07 (Q91V76) and similar to hypothetical protein 4833421E05Rik (XP_216665) that were previously predicted from nucleic acid sequences. Since RIKEN cDNA 4931406C07 shows 94.3% identity to hypothetical LOC363016 and XP_216665 was not identified with MS/MS analysis, we applied two hypothetical proteins, HP Q8CC88 and hypothetical LOC363016 for further bioinformatic characterization.

Table 3 describes comparable sequence alignment results of two HPs using Blastp, PSI-blast, RPS-blast, FASTA, and MP searches. HP Q8CC88 is 20.3−21.0% identical to Midasin protein family and hypothetical LOC363016 shows 86% sequence identity to PTD012 protein which is not characterized.

To characterize tentative function of these HPs, different database searches (InterPro, ELM, ScanProsite, Interweaver, STRING, SignalP, and PSORTII) were performed for examining functional domains, motifs and protein−protein interactions (Table 4). On the basis of bioinformatic searches with the partial peptide sequences observed by MS and MS/MS (Figure 6 and Supplementary Table 1 online), HP Q8CC88 showed similarity to AAA (ATPases associated with diverse cellular activities) protein family. STRING-database search results predicted the interaction of HP Q8CC88 with different proteins such as dsRNA-specific ribonuclease, guanylate kinase, ATPases involved in chromosome partitioning, RNA binding proteins, Myb superfamily proteins, predicted GTPases, predicted NTPase (NACHT family) and serine/threonine protein kinase. Several interacting proteins in *Drosophila melanogaster* and Baker's yeast were predicted by InterWeaver search. CG6363-PA

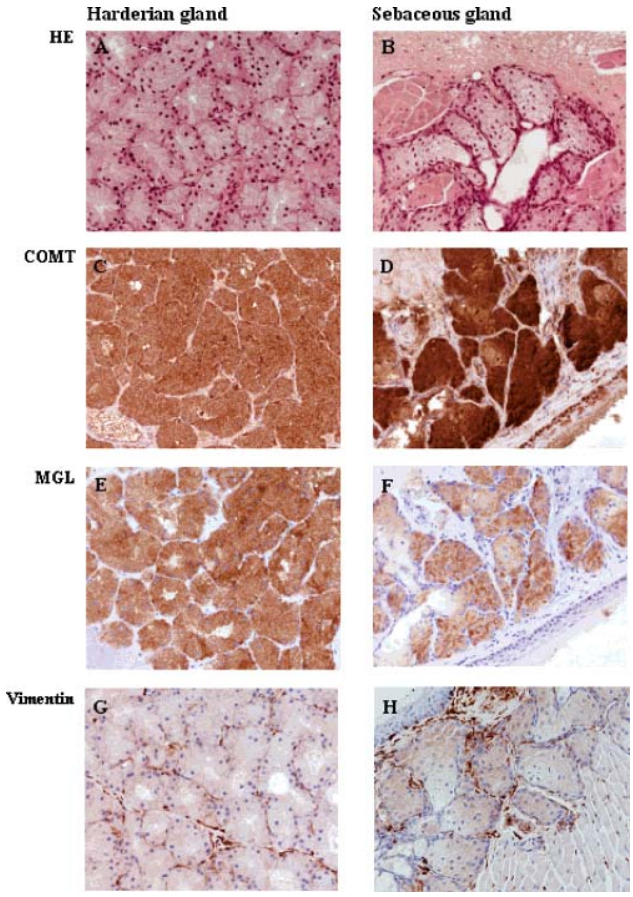

Figure 4. (A,B) Hematoxylin-eosin stain of the rat HG (A) and sebaceous gland (B) (×200). C−H: Immunohistochemistry for COMT (C,D), MGL (E,F) and vimentin (G,H) in the rat Harderian gland (left) and sebaceous gland (right) (all × 200). Both glands show strong immunoreactivity for COMT and MGL in epithelial cells. Vimentin is only expressed in mesenchymal tissue (vessel walls, fibroblast), whereas epithelial cells remain negative.

(NP_650442) and CG11581-PA (NP_572940) were potential interacting partners of HP Q8CC88 in *Drosophila melanogaster* and probable membrane protein YG245c-yeast (S64571), histone H4 (gi 70775), U1 SNP1-associating protein 1 (Q03714), ESS1 protein and 26S protease regulatory subunit 6B homologue (P33298) were some examples for the predicted interacting partners of HP Q8CC88 in yeast.

PROSITE-database predicted results identified 6 different motifs for hypothetical LOC363016 (Table 4). A bacterial adhesion domain, important for receptor binding to host cells during pathogenicity of bacteria[36] was identified using InterPro database. This domain consists of beta-sandwich formed sheets with a Greek-key topology and represents a subclass of the immunoglobulin-like fold (InterPro). Protein−protein interaction database searches (InterWeaver and STRING) predicted different interacting partner for hypothetical LOC363016. Based on STRING-database search result, cytochrome P450 subfamily, 17 beta-hydrogenase type 3, Aldehyde dehydrogenase, mitochondrial oxoglutarate/malate carrier proteins, peroxidase/oxygenase, formyltetrahydrofolate synthetase, acetyl-CoA acetyltransferase, actin regulatory proteins (gelsolin/villin family), predicted membrane protein (patched superfamily), and phos-

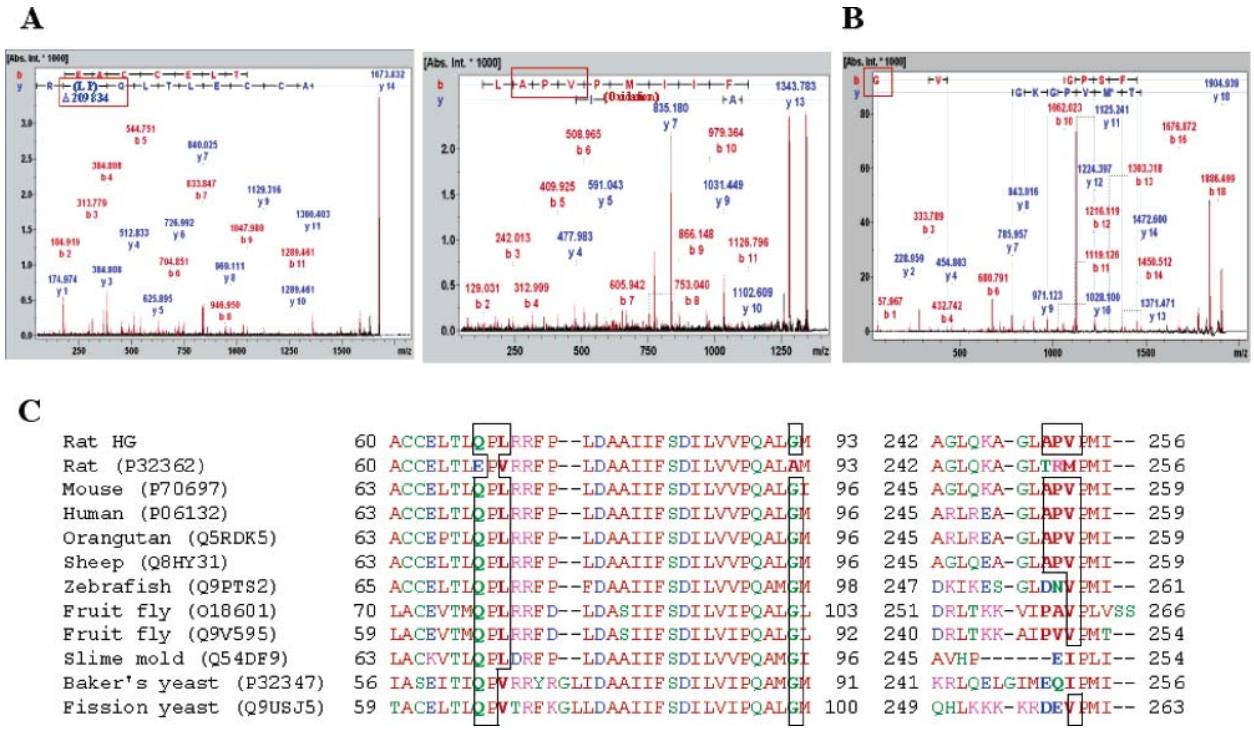

Figure 5. Conflict sequences of URO-D in the rat HG analyzed by MALDI−MS/MS. Two trypsin digested peptides show 5 amino acids sequence conflicts (boxed) with LIFT-TOF/TOF spectra of the precursor ion detected at *m/z* 1673 and 1343 (A) and one chymotrypsin digested peptide contains one conflict (boxed) in URO-D in the rat HG (B). Comparison of URO-D in the rat HG with those from rat and other species (C). The part of sequence alignment where sequence conflicts (in box) were observed is demonstrated and the complete alignment is provided as Supporting Information Figure 4 online.

Table 2. Identification of Uroporphyrinogen Decarboxylase (URO-D) in the Rat HG Using 3 Different Enzymes

				MS/MS results							
enzyme	matches[a]	score[b]	seq (%)	observed[c]	M_r (expt)[d]	M_r (calc)[e]	miss[f]	score[g]	expect[h]	peptide[i]	mode
trypsin	16	422	38.2	824.41	823.41	823.42	0			YLPEFR	de Novo
				879.49	878.48	878.50	0	39	0.0059	K.FALPYIR.D	LID
				879.53	878.52	878.50	0	(28)	0.016	K.FALPYIR.D	CID
				1202.54	1201.53	1201.52	0	61	1.8e-005	R.AAQDFFSTCR.S	LID
				1413.74	1412.73	1412.70	1	38	0.008	K.GPSFPEPLREER.D	LID
				1545.81	1544.80	1544.78	0	96	1.3e-008	R.LVQQMLNDFGPQR.Y	LID
				2122.12	2121.11	2121.11	0	37	0.0064	R.DPAAVASELGYVFQAITLTR.Q	LID
				2391.31	2390.30	2390.30	1	92	1.2e-008	R.LRDPAAVASELGYVFQAITLTR.Q	LID
				2391.32	2390.31	2390.30	1	(46)	0.000 44	R.LRDPAAVASELGYVFQAITLTR.Q	CID
				1343.79	1342.78	1342.77	0	31	0.015	K.AGL**APV**PMIIFAK.D + M_{Ox}	LID
				1673.82	1672.81	1672.79	0	(51)	0.000 46	R.SPEACCELTLQPLR.R	CID
				1673.82	1672.81	1672.79	0	51	0.000 46	R.SPEACCELTLQ**PLR**.R	LID
chymo-trypsin	21	256	37.8	1318.76	1317.75	1317.76	1	59	0.000 24	L.RRFPLDAAIIF.S	LID
				1618.82	1617.81	1617.80	1	22	1.7	Y.ASEEEIGRLVQQML.D + M_{Ox}	LID
				1726.87	1725.86	1725.85	2	46	0.0058	Y.LPEFRETRAAQDFF.S	LID
				1904.93	1903.92	1903.91	0	55	0.0007	L.**G**MEVTMVPGKGPSFPEPL.*R* + 2 M_{Ox}	LID
				2169.02	2168.02	2168.00	2	60	0.000 19	Y.IANLGHGLYPDMDPEHVGAF.L + M_{Ox}	LID
Asp-N	4	92	17	1395.70	1394.69	1394.65	0	49	0.000 41	N.DTFLRAAWGEET.D	LID

[a] Matched peptide numbers from Mascot database searching results. [b] Mascot score is −10*Log (*P*), where *P* is the probability that the observed match is a random event (MASCOT, http://www.matrixscience.com/help/scoring-help.html). [c] Experimental *m/z* value. [d] Experimental *m/z* transformed to a relative molecular mass. [e] Calculated relative molecular mass of the matched peptide. [f] Number of missed enzyme cleavage sites. [g] Ions score − if there are duplicate matches to the same peptide, then the CID scoring matches are shown in brackets. [h] Expectation value for the peptide match. (The number of times we would expect to obtain an equal or higher score, purely by chance. The lower this value, the more significant the result). [i] M_{Ox}, Oxidation (M).

phatidylinositol 4-kinase were identified confidently as potential interacting partners of this HP. InterWeaver search predicted two interacting proteins CG5271-PA (NP_476778) and CG9119-PA (NP_612081) in *Drosophila* melanogaster for hypothetical LOC363016. With RPS−BLAST search, however, no conserved domain was identified for this HP and 3D homology modeling server and Phyre could not introduce any reliable 3D model for prediction of 3D model of this protein.

ATPase Activity of HP Q8CC88. HP Q8CC88 from three independent experiments was eluted from 2D gel and renatured to confirm ATPase activity which was predicted from bioinformatic tools (Table 4). Proteins were serially diluted for

Table 3. Sequence Alignment Search Results of Hypothetical Proteins in the Rat HG

acc. no.	protein name	blastp	PSI-blast	RPS-blast	FASTA	MPsearch
Q8CC88	*Mus musculus* adult male cecum cDNA, RIKEN full-length enriched library, clone:9130206H04 product:hypothetical P-loop containing nucleotide triphosphate hydrolases structure containing protein full insert sequence	midasin [human] (Q9NU22) score: 79.3 bits (194), expect: 6e-14 identities: 152/709 (21%), positives: 284/709 (40%), gaps: 90/222 (12%)	midasin [human] (Q9NU22) score: 71.2 bits (173), expect: 2e-11 identities: 169/788 (21%), positives: 312/788 (39%), gaps: 113/788 (14%)	pfam06383, P_denitri_CobS, Cobalamin biosynthesis protein CobS. CD-Length: 328 residues, score: 40.1 bits (93), expect: 0.001	midasin (MIDAS-containing pr) (Q12019) − 4910 aainitn: 269 init1: 107 opt: 224 *Z*-score: 224.6 bits: 55.2 E(): 0.00023 Smith-Waterman score: 245; 20.370% identity (24.160% ungapped) in 918 aa overlap (138−990:791−1629)	C12.2 [Fragment] (Q9NHX8) (769 AA) score 2628 match 47.1% matches 352 conservative 180 mismatches 187 indels 29 gaps 22
Q5U2Q3	hypothetical LOC363016	PTD012 [*Homo sapiens*] (CAG38569) score = 576 bits (1484), expect = 4e-163, identities = 271/315 (86%), positives = 292/315 (92%), gaps = 0/315 (0%)	PTD012 protein [*Homo sapiens*] (AAH07110) score = 548 bits (1412), Expect = 9e-155, method: Composition-based stats. identities = 257/297 (86%), positives = 278/297 (93%), gaps = 0/297 (0%)	no hit	PTD012 (Q) (Q6FI88) −315 aa initn: 1911 init1: 1911 opt: 1911 Z-score: 2334.0 bits: 440.0 E(): 9.4e-122 Smith-Waterman score: 1911; 86.032% identity (86.032% ungapped) in 315 aa overlap (1−315:1−315)	PTD012 (Q) (Q6FI88) (315 aa) score 2450 match 86.0% matches 271 conservative 20 mismatches 24 indels 0 gaps 0

the determination of the suitable enzyme activity in the linear range at 25 °C with a colorimetric method to measure the released inorganic phosphate (P_i) by ATPase hydrolysis (Figure 7A). With a standard curve for P_i, ATPase activity was calculated and showed 0.0762 ± 0.0087 U/min; one unit is the amount of enzyme that catalyses the reaction of 1 μmol of substrate per minute. To determine thermal stability, ATPase activity was measured at different temperatures and the maximum of activity was shown to be at about 80 °C and sustained at 100 °C (Figure 7B).

Discussion

In this study the major findings were identification of HG proteins from lipid and porphyrin metabolism, but also a series of other pathways, interesting individual proteins, and some were never described at the protein chemical level before. Moreover, database sequence conflicts were solved and a reference database of more than 300 different gene products with many individual expression forms was provided that forms the basis for future protein analytical studies on this interesting organ.

Thirty-three proteins involved in lipid metabolism from rat HG were observed and indeed, there is limited data on proteins for lipid handling and metabolism. As shown above, there is significant information about lipids although there is limited data to show specific function of lipids in HG.[2]

There are 111 known fatty acid-binding proteins from different species with six isoforms: adipocyte- (A-FABP), brain- (B-FABP), epidermal-(E-FABP), heart- (H-FABP), intestinal-(I-FABP) and liver-specific FABP (L-FABP) involved in fatty acid uptake, transport, targeting, and modulating fatty acid concentration (http://www.expasy.org/cgi-bin/get-similar?name=fatty-acid%20binding%20protein%20(FABP)%20family). FABP in the armadillo HG was reported for the first time in 1998 and suggested the presence of the heart-specific type of FABP by partial amino acid sequencing using Edman degradation after the sequence alignment.[37] In this study, we identified two spots of FABP and MS/MS data unambiguously assigned both protein spots to epidermal type isoforms of FABP (E-FABP) (see Supporting Information Figure 4 online). It is, however, possible that H-FABP was not detectable as a high abundance protein using our technique but the expression of E-FABP seems to be the predominant isoform in the rat HG due to its high abundance. Simply from inspection the abundance of E-FABP is also higher in HG than those of EABP in rat primary neurons (E- and H-FABP) and astrocytes (E-FABP),[37] rat hippocampus (E-FABP),[38] and human hippocampus (E- and B-FABP),[39] based on previously constructed ref 2D maps using a comparable proteomics method.

The presence of some of lipid metabolic proteins was confirmed by Western blot analysis. The same expression pattern of AOX was shown between MALDI analysis and 2D-Western blot data with two protein spots at approximately 48 kDa. Five spots of SCP2 at 58 kDa were identified by both MALDI and 2D-Western blot analyses but two spots at 44 kDa identified by MALDI−MS were not detected by Western blot. There was no matched tryptic peptide mass at the C-terminus (residues 405−547) from two spots at 44 kDa, whereas peptide masses representing the C-terminus were observed in other SCP2 spots at 58 kDa (see Supporting Information Figure 4 online). These fragment forms were not detected by Western blot because the antibody against SCP2 recognizes the C-terminus (residues 405−547) from the immature (58 kDa) and mature form (13 kDa).[33] This is a good example to show the advantage of combining immunochemistry with proteomics technique for the identification of protein isoforms.

Table 4. Functional Characterization of Hypothetical Proteins in the Rat HG

accession no.	protein name	gene name	domain	motif	subcellular localizatin	signal peptide
Q8CC88	*Mus musculus* adult male cecum cDNA, RIKEN full-length enriched library, clone:9130206H04 product:hypothetical P-loop containing nucleotide triphosphate hydrolases structure containing protein, full insert sequence	1300010F03Rik	AAA ATPase domain (InterPro: IPR003593) ATPase associated with various cellular activities (Pfam: PF07728 InterPro: IPR011704)	N-myrisoylation site (PROSITE: PS00008) protein kinase C phosphorylation site (PROSITE: PS00005) casein kinase II phosphorylation site (PROSITE: PS00006) N-glycosylation site (PROSITE: PS00001) ATP/GTP-binding site motif A (P-loop) (PROSITE: PS00017) tyrosine kinase phosphorylation site (PROSITE: PS00007) cAMP- and cGMP-dependent protein kinase phosphorylation site (PROSITE: PS00004) amidation site (PROSITE: PS00009) tyrosine sulfation site (PROSITE: PS00003)	cytoplasm	nonsecretory protein
Q5U2Q3	hypothetical LOC363016	RGD1309534_ predicted	bacterial adhesion domain (InterPro: IPR008966, Supfam: SSF494901)	N-myrisoylation site (PROSITE: PS00008) casein kinase II phosphorylation site (PROSITE: PS00006) N-glycosylation site (PROSITE: PS00001) protein kinase C phosphorylation site (PROSITE: PS00005) cAMP- and cGMP-dependent protein kinase phosphorylation site (PROSITE: PS00004) tyrosine kinase phosphorylation site (PROSITE: PS00007)	cytoplasm	nonsecretory protein

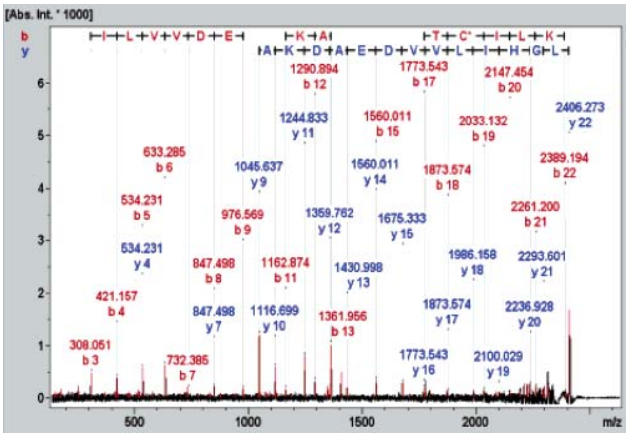

Figure 6. LIFT-TOF/TOF spectrum of the precursor ion detected at *m/z* 2406.287 in HP Q8CC88. The identified sequence LGHILVVDEADKAPTNVTCILK represents the presence of Walker B2 motif in HP Q8CC88.

MGL is participating in the last step of triglyceride lipolysis to convert monoacylglycerides to free fatty acids and glycerol and is involved in neuronal 2-arachidonoylglycerol inactivation.[40] Demonstration of several isoforms on 2D gel was revealed and the presence of this key enzyme was confirmed by immunoblotting. Immunohistochemistry revealed parenchymatous staining showing the abundant expression in this gland.

Thyroid hormone-inducible hepatic protein (syn.: spot 14) is involved in tissue specific regulation of lipogenesis and tumor metabolism.[41] Spot 14 is known for the exclusive expression in lipogenic tissues such as liver, adipose tissue and lactating mammary gland[41,42] and we observed this protein in HG as a single spot. In tumor metabolism, spot 14 was proposed as a modulator of tumorigenesis from the fact that it inhibited cell proliferation and induced cell differentiation and cell death in a human breast cancer cell line.[43] Another tumor related protein, tumor suppressor protein HIV-1 tat interactive protein 2 [44] was unambiguously identified in HG as a single spot. The biological meaning of the presence of high abundance tumor-related proteins remains open.

Scinderin, a novel Ca^{2+}-activated actin filament-severing protein, shows restricted tissue distribution and the protein is, e.g., expressed in the adrenal medulla, brain, pituitary, kidney, salivary gland, and testis but is not present in liver, plasma, skeletal and heart muscles while another Ca^{2+}-dependent actin

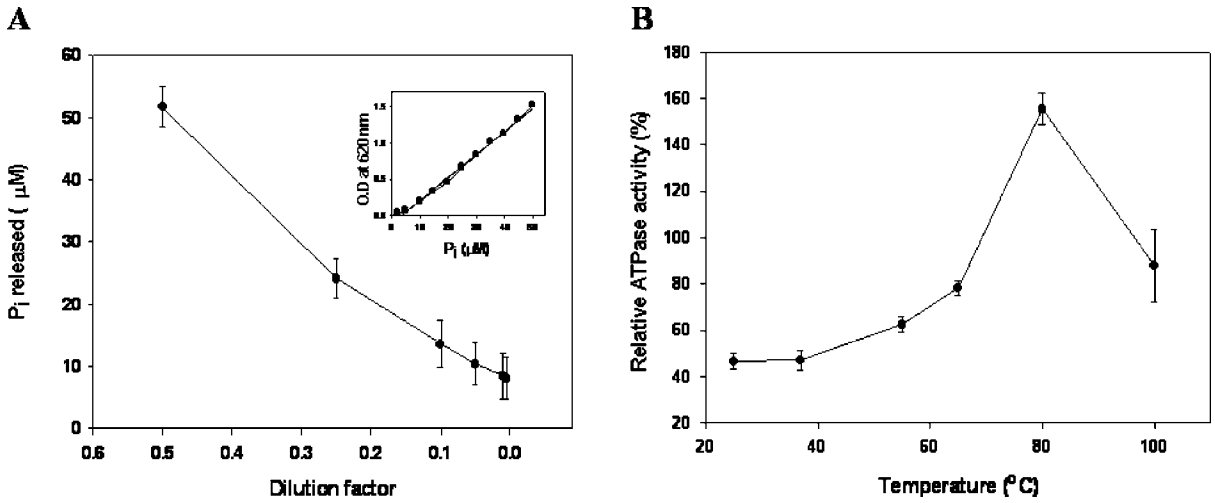

Figure 7. ATPase activity in HP Q8CC88 recovered from 2D gel. ATPase activity of Q8CC88 at serial diluted protein concentrations at 25 °C (inset: standard curve for P_i to calculate enzyme activity) (A). Effect of temperature on the ATPase activity of HP Q8CC88 (B).

filament-severing protein, gelsolin reveals ubiquitous tissue distribution.[45] It is shown herein that HG scinderin is a high abundant protein and represented by three spots with different p*I*s probably reflecting the presence of post-translational modifications whereas gelsolin was not observed (see Supporting Information Table 1 online), which may indicate that scinderin is acting as a major actin severing protein in the rat HG.[46,47]

Distribution of COMT in rat tissues was reported and showed expression in most rat organs except for the HG.[48] According to apparent molecular weights, two transcriptional products of COMT, a band probably representing the soluble (S-COMT) and probably a membrane bound form (M-COMT) in rat HG were demonstrated by Western blot but two forms of S-COMT were detected on 2DE with subsequent MALDI TOF/TOF analysis: The potential signal-anchor sequence for type II membrane protein (LAAVSLGLLLLALLLLL) from the rat HG (http://www.expasy.org/uniprot/P22734) was not identified and therefore two forms of S-COMT rather than a M-COMT were detected. As no specific antibody is available, mass spectrometry based analysis may be useful to distinguish the two isoforms by analysis of the M-COMT partial sequence. On the basis of the protein levels revealed by Western blot, one S-COMT band was dominant in the rat HG. In other tissues, such as liver, kidney and gastrointestinal tract 70% of total COMT are of the M-COMT type and 30% of the S-COMT type.[49] On the basis of the statement above, these findings may be revisited by mass spectrometrical techniques. Abundant expression in HG may indicate that monoaminergic may be a major neurotransmission system in HG.

Porphyrins are another major secretory product of the HG. It has been shown that the golden hamster HG possesses all the enzymes involved in porphyrin synthesis.[1,50] In the present study, five key enzymes of porphyrin biosynthesis in the rat HG were detected: 5-aminolevulinate synthase (P13195, with four spots), delta-aminolevulinic acid dehydratase (P06214, with two spots), porphobilinogen deaminase (P19356, as a single spot), uroporphyrinogen-III synthase (P51163, as a single spot) and uroporphyrinogen decarboxylase (URO-D; P32362, with two spots) (see Supporting Information Table 1 online). Among them, URO-D converts uroporphyrinogen to coproporphyrinogen by decarboxylation of the four acetic acid side chains.[51] Although amino acids sequence of rat URO-D was predicted from the nucleotide in 1987,[52] it has not been characterized at the protein level. Several sequence conflicts of URO-D in rat HG in the Swiss-Prot database could be solved herein. Six amino acids were observed as different from the rat protein database by MS/MS analysis and sequences were shown as conserved by sequence alignment with URO-D in other taxonomies (Figure 5 and Supporting Information Figure 5 online). This finding identifies mass spectrometrical analysis as a fast and powerful method for protein identification with robust sequence information.

MALDI-TOF/TOF and database searches showed the existence of HPs at the protein level in the HG. HP Q8CC88 protein was predicted to contain an AAA ATPase domain (Table 4) and indeed MS analysis identified the corresponding peptide sequence. An approach to determine ATPase activity directly from the excised protein spot was successful and provides evidence for functional relevance of this protein (Figure 7). The method to identify a protein, extract and renature the spot followed by determination of its activity is an intriguing finding that may have analytical implications for the future extending applications of the proteomics method. An excursion on the corresponding ATPase superfamily, necessary to understand the context is provided in Supporting Information (online).

In this study, we presented for the first time a comprehensive 2D map of rat HG proteins with almost seven hundred spots representing 304 individual proteins. Key protein elements for lipid metabolism, handling and porphyrin synthesis were identified and immunoblottings including 2D-Western blots were performed to verify the expression of some proteins identified by mass spectrometry. We show the potential of the method to solving database conflicts as in the case of URO-D and show the existence of the HP Q8CC88 predicted from the nucleic acid sequence. The use of bioinformatics led to prediction of conformation and tentative function and indeed, the proposed ATPase activity was confirmed by enzyme activity assay using an extracted gel spot following renaturation. The fact that we observed vimentin but that this protein was

expressed in connective tissue rather than in HG epithelial cells shows the importance of immunohistochemistry in the area. The methodology used is suggested an useful analytical tool for several applications.

Acknowledgment. We thank Prof. Dr. K. Wirtz (Utrecht, Netherlands) and Dr. G. Hoefler (Graz, Austria) for providing antibodies.

Supporting Information Available: Unambiguously identified proteins in the rat HG with MALDI−MS/MS analysis (Supporting Information Table 1 and Supporting Information Figure 2). One MS/MS spectrum at *m*/*z* 3291 in identified APMAP, which could not be assigned using Mascot database search (Supporting Information Figure 3). Identified proteins in the rat HG categorized into several functional groups based on their representative biological roles (Supporting Information Table 1). Confirmed expression of MGL in HG by Western blot analysis. MGL observed at 31 and 35 kDa in agreement with MALDI-TOF/TOF result (Supporting Information Figure 4). Highly expressed epidermal-type fatty acid-binding protein (E-FABP; P55053), which has not been described in the HG, on 2D gel from the rat HG by MALDI−MS/MS (Supporting Information Table 1 and Supporting Information Figure 2). Six out of nine peptides assigned in rat URO-D and 2 MS/MS results not assigned with database in rat taxonomy (Supporting Information Figure 5). Two spots of FABP and MS/MS data unambiguously assigned both protein spots to epidermal type isoforms of FABP (E-FABP) (Supporting Information Figure 4). This material is available free of charge via the Internet at http://pubs.acs.org.

References

(1) Payne, A. P. The harderian gland: a tercentennial review. *J. Anat.* **1994**, *185*, 1−49.
(2) Buzzell, G. R. The Harderian gland: perspectives. *Microsc. Res. Technol.* **1996**, *34*, 2−5.
(3) Villapando, I.; Ramirez, M.; Zepeda-Rodriguez, A.; Castro, A. C.; Cardenas-Vazquez, R.; Vilchis, F. The Harderian gland of the Mexican volcano mouse Neotomodon alstoni alstoni (Merriam 1898): a morphological and biochemical approach. *J. Exp. Zoolog. A. Comput. Exp. Biol.* **2005**, *303*, 13−25.
(4) Shanas, U.; Terkel, J. Grooming secretions and seasonal adaptations in the blind mole rat (*Spalax ehrenbergi*). *Physiol. Behav.* **1996**, *60*, 653−656.
(5) Thiessen, D. D. Body temperature and grooming in the Mongolian gerbil. *Ann. N.Y. Acad. Sci.* **1988**, *525*, 27−39.
(6) Sakai, T.; Yohro, T. A histological study of the Harderian gland of Mongolian gerbils, *Meriones meridianus*. *Anat. Rec.* **1981**, *200*, 259−270.
(7) Hais, I. M.; Strych, A.; Chmelar, V. Preliminary thin-layer chromatographic characterization of the rat Harderian gland lipid. *J. Chromatogr.* **1968**, *35*, 179−191.
(8) Kahan, I. L.; Juhasz, K.; Mindszenti, S. Lipids of the Harderian gland of rabbits. *Acta Biol. Acad. Sci. Hung.* **1967**, *18*, 295−301.
(9) Blank, M. L.; Kasama, K.; Snyder, F. Isolation and identification of an alkyldiacylglycerol containing isovaleric acid. *J. Lipid Res.* **1972**, *13*, 390−395.
(10) Murawski, U.; Jost, U. Unsaturated wax esters in the Harderian gland of the rat. *Chem. Phys. Lipids* **1974**, *13*, 155−158.
(11) Bareggi, R.; Narducci-Bareggi, P.; Crescenzi, A. Lipids in the Harder's gland of certain rodents. III: Glycolipids. *Basic Appl. Histochem.* **1979**, *23*, 165−169.
(12) Bareggi, R.; Crescenzi, A.; Narducci-Bareggi, P. Lipids in the Harder's gland of certain rodents. II: Phospholipids. Basic *Basic Appl. Histochem.* **1979**, *23*, 161−163.
(13) Bareggi, R.; Crescenzi, A.; Narducci-Bareggi, P. Lipids in the Harder's gland of certain rodents. I: Neutral lipids. *Basic Appl. Histochem.* **1979**, *23*, 155−160.
(14) Tvrzicka, E.; Rezanka, T.; Krijt, J.; Janousek, V. Identification of very-long-chain fatty acids in rat and mouse harderian gland lipids by capillary gas chromatography−mass spectrometry. *J. Chromatogr.* **1988**, *431*, 231−238.
(15) Harvey, D. J. Identification by gas chromatography and mass spectrometry of lipids from the rat Harderian gland. *J. Chromatogr.* **1991**, *565*, 27−34.
(16) Antolin, I.; Uria, H.; Tolivia, D.; Rodriguez-Colunga, M. J.; Rodriguez, C.; Kotler, M. L.; Menendez-Pelaez, A. Porphyrin accumulation in the harderian glands of female Syrian hamster results in mitochondrial damage and cell death. *Anat. Rec.* **1994**, *239*, 349−359.
(17) Park, S. H.; Satoh, Y.; Kumagai, S.; Seyama, Y. Localization of porphyrin in mouse Harderian glands. *Arch. Histol. Cytol.* **1996**, *59*, 189−195.
(18) Spike, R. C.; Payne, A. P.; Thompson, G. G.; Moore, M. R. High-performance liquid chromatographic analyses of porphyrins in hamster Harderian glands. *Biochim. Biophys. Acta* **1990**, *1034*, 1−3.
(19) Lim, C. K.; Razzaque, M. A.; Luo, J.; Farmer, P. B. Isolation and characterization of protoporphyrin glycoconjugates from rat harderian gland by HPLC, capillary electrophoresis, and HPLC/electrospray ionization MS. *Biochem. J.* **2000**, *347*, 757−761.
(20) Buzzell, G. R.; Menendez-Pelaez, A.; Hoffman, R. A.; Rodriguez, C.; Antolin, I. rogenic control of porphyrin in the Harderian glands of the male Syrian hamster is modulated by the photoperiod, which suggests that the sexual differences in porphyrin concentrations in this gland are important functionally. *Anat. Rec.* **1994**, *240*, 52−58.
(21) Marr, F. A.; Shah, S. W.; McGadey, J.; Moore, M. R.; Houston, T.; Payne, A. P. The effects of bromocriptine and prolactin on porphyrin biosynthesis in the harderian gland of the male hamster, *Mesocritecus auratus*. *J. Comput. Physiol. B* **1995**, *164*, 524−529.
(22) Rodriguez-Colunga, M. J.; Fernandez, C.; Antolin, I.; Rodriguez, C.; Tolivia, D.; Menendez-Pelaez, A. Chronic administration of melatonin induces changes in porphyrins and in the histology of male and female hamster harderian gland: interrelation with the gonadal status. *J. Pineal Res.* **1991**, *11*, 42−48.
(23) Payne, A. P.; Shah, S. W.; Marr, F. A.; McGadey, J.; Thompson, G. G.; Moore, M. R. Hormones and the control of porphyrin biosynthesis and structure in the hamster harderian gland. *Microsc. Res. Technol.* **1996**, *34*, 123−132.
(24) Kajimura, T.; Satoh, H.; Watanabe, G.; Taya, K. Effect of hyperprolactinemia induced by pituitary grafts or castration on porphyrin content of the mouse Harderian gland. *J. Toxicol. Sci.* **2001**, *26*, 151−161.
(25) Tomas-Zapico, C.; Coto-Montes, A.; Martinez-Fraga, J.; Rodriguez-Colunga, M. J.; Tolivia, D. Effects of continuous light exposure on antioxidant enzymes, porphyric enzymes and cellular damage in the Harderian gland of the Syrian hamster. *J. Pineal Res.* **2003**, *34*, 60−68.
(26) Shirama, K.; Kohda, M.; Kohda, M.; Hokano, M. Effects of lighting conditions and of hormone replacement on the level of porphyrins in the rat Harderian gland. *J. Endocrinol. Invest.* **1987**, *10*, 79−82.
(27) Yang, J. W.; Rodrigo, R.; Felipo, V.; Lubec, G. Proteome analysis of primary neurons and astrocytes from rat cerebellum. *J. Proteome Res.* **2005**, *4*, 768−788.
(28) Suckau, D.; Resemann, A.; Schuerenberg, M.; Hufnagel, P.; Franzen, J.; Holle, A. A novel MALDI LIFT-TOF/TOF mass spectrometer for proteomics. *Anal. Bioanal. Chem.* **2003**, *376*, 952−965.
(29) Macht, M.; Asperger, A.; Deininger, S. O. Comparison of laser-induced dissociation and high-energy collision-induced dissociation using matrix-assisted laser desorption/ionization tandem time-of-flight (MALDI-TOF/TOF) for peptide and protein identification. *Rapid Commun. Mass Spectrom.* **2004**, *18*, 2093−2105.
(30) Shevchenko, A.; Sunyaev, S.; Loboda, A.; Shevchenko, A.; Bork, P.; Ens, W.; Standing, K. G. Charting the proteomes of organisms with unsequenced genomes by MALDI-quadrupole time-of-flight mass spectrometry and BLAST homology searching. *Anal. Chem.* **2001**, *73*, 1917−1926.
(31) Lubec, G.; Afjehi-Sadat, L.; Yang, J. W.; John, J. P. Searching for hypothetical proteins: theory and practice based upon original data and literature. *Prog. Neurobiol.* **2005**, *77*, 90−127.
(32) Albrektsen, T.; Richter, H. E.; Clausen, J. T.; Fleckner, J. Identification of a novel integral plasma membrane protein induced during adipocyte differentiation. *Biochem. J.* **2001**, *359*, 393−402.
(33) Ossendorp, B. C.; Voorhout, W. F.; van Amerongen, A.; Brunink, F.; Batenburg, J. J.; Wirtz, K. W. Tissue-specific distribution of a peroxisomal 46-kDa protein related to the 58-kDa protein (sterol carrier protein x; sterol carrier protein 2/3-oxoacyl-CoA thiolase). *Arch. Biochem. Biophys.* **1996**, *334*, 251−260.

(34) Nohammer, C.; El-Shabrawi, Y.; Schauer, S.; Hiden, M.; Berger, J.; Forss-Petter, S.; Winter, E.; Eferl, R.; Zechner, R.; Hoefler, G. cDNA cloning and analysis of tissue-specific expression of mouse peroxisomal straight-chain acyl-CoA oxidase. *Eur. J. Biochem.* **2000**, *267*, 1254−1260.
(35) Lanzetta, P. A.; Alvarez, L. J.; Reinach, P. S.; Candia, O. A. An improved assay for nanomole amounts of inorganic phosphate. *Anal. Biochem.* **1979**, *100*, 95−97.
(36) Dodson, K. W.; Pinkner, J. S.; Rose, T.; Magnusson, G.; Hultgren, S. J.; Waksman, G. Structural basis of the interaction of the pyelonephritic, E. coli adhesin to its human kidney receptor. *Cell* **2001**, *105*, 733−743.
(37) Cavagnari, B. M.; Cordoba, O. L.; Veerkamp, J. H.; Santome, J. A.; Affanni, J. M. Presence of a fatty acid-binding protein in the armadillo Harderian gland. *Int. J. Biochem. Cell Biol.* **1998**, *30*, 465−473.
(38) Fountoulakis, M.; Tsangaris, G. T.; Maris, A.; Lubec, G. The rat brain hippocampus proteome. *J. Chromatogr. B Anal. Technol. Biomed. Life Sci.* **2005**, *819*, 115−129.
(39) Yang, J. W.; Czech, T.; Lubec, G. Proteomic profiling of human hippocampus. *Electrophoresis* **2004**, *25*, 1169−1174.
(40) Dinh, T. P.; Carpenter, D.; Leslie, F. M.; Freund, T. F.; Katona, I.; Sensi, S. L.; Kathuria, S.; Piomelli, D. Brain monoglyceride lipase participating in endocannabinoid inactivation. *Proc. Natl. Acad. Sci. U.S.A.* **2002**, *99*, 10819−10824.
(41) Moncur, J. T.; Park, J. P.; Memoli, V. A.; Mohandas, T. K.; Kinlaw, W. B. The "Spot 14" gene resides on the telomeric end of the 11q13 amplicon and is expressed in lipogenic breast cancers: implications for control of tumor metabolism. *Proc. Natl. Acad. Sci. U.S.A.* **1998**, *95*, 6989−6994.
(42) Zhu, Q.; Anderson, G. W.; Mucha, G. T.; Parks, E. J.; Metkowski, J. K.; Mariash, C. N. The Spot 14 protein is required for de novo lipid synthesis in the lactating mammary gland. *Endocrinology* **2005**, *146*, 3343−3350.
(43) Sanchez-Rodriguez, J.; Kaninda-Tshilumbu, J. P.; Santos, A.; Perez-Castillo, A. The spot 14 protein inhibits growth and induces differentiation and cell death of human MCF-7 breast cancer cells. *Biochem. J.* **2005**, *390*, 57−65.
(44) Ito, M.; Jiang, C.; Krumm, K.; Zhang, X.; Pecha, J.; Zhao, J.; Guo, Y.; Roeder, R. G.; Xiao, H. TIP30 deficiency increases susceptibility to tumorigenesis. *Cancer Res.* **2003**, *63*, 8763−8767.
(45) Tchakarov, L.; Vitale, M. L.; Jeyapragasan, M.; Rodriguez Del Castillo, A.; Trifaro, J. M. Expression of scinderin, an actin filament-severing protein, in different tissues. *FEBS Lett.* **1990**, *268*, 209−212.
(46) Rodriguez Del Castillo, A.; Lemaire, S.; Tchakarov, L.; Jeyapragasan, M.; Doucet, J. P.; Vitale, M. L.; Trifaro, J. M. Chromaffin cell scinderin, a novel calcium-dependent actin filament-severing protein. *EMBO J.* **1990**, *9*, 43−52.
(47) Silacci, P.; Mazzolai, L.; Gauci, C.; Stergiopulos, N.; Yin, H. L.; Hayoz, D. Gelsolin superfamily proteins: key regulators of cellular functions. *Cell. Mol. Life Sci.* **2004**, *61*, 2614−2623.
(48) Karhunen, T.; Tilgmann, C.; Ulmanen, I.; Julkunen, I.; Panula, P. Distribution of catechol-O-methyltransferase enzyme in rat tissues. *J. Histochem. Cytochem.* **1994**, *42*, 1079−1090.
(49) Zhu, B. T. Catechol-O-Methyltransferase (COMT)-mediated methylation metabolism of endogenous bioactive catechols and modulation by endobiotics and xenobiotics: importance in pathophysiology and pathogenesis. *Curr. Drug Metab.* **2002**, *3*, 321−349.
(50) Thompson, G. G.; Hordovatzi, X.; Moore, M. R.; McGadey, J.; Payne, A. P. Sex differences in haem biosynthesis and porphyrin content in the Harderian gland of the golden hamster. *Int. J. Biochem.* **1984**, *16*, 849−852.
(51) Jones, M. A.; Thientanavanich, P.; Anderson, M. D.; Lash, T. D. Comparison of two assay methods for activities of uroporphyrinogen decarboxylase and coproporphyrinogen oxidase. *J. Biochem. Biophys. Methods* **2003**, *55*, 241−249.
(52) Romana, M.; Le Boulch, P.; Romeo, P. H. Rat uroporphyrinogen decarboxylase cDNA: nucleotide sequence and comparison to human uroporphyrinogen decarboxylase. *Nucleic Acids Res.* **1987**, *15*, 7211.

PR060082B